

# **Results of hydraulic tests performed before and after stimulation of the three test cells in Kluczewo, Poland**

Deliverable D5 and D14

Nilsson, B., Amfelt, M., Tsakiroglou, C., Kasela, T., Gosk, E.



# Results of hydraulic tests performed before and after stimulation of the three test cells in Kluczewo, Poland

Deliverable D5 and D14

Nilsson, B., Tsakiroglou, C., Haeseler, F., Kasela, T., Klint, K.E.,  
Gosk, E., Brøker, T., Slack, B. & Murdoch, L.



# ABOUT THIS DOCUMENT

This report is a joint report of the deliverables D5 and D14 of the Stresoil Project.

---

Title	Deliverable D5 and D14. Results of hydraulic tests performed before and after stimulation of the three test cells in Kluczewo, Poland
-------	---

---

Purpose	Joint report of the deliverables D5 & D14 to EU in relation to Contract No. SSPI-CT-2003-004017
Filename	Stresoil-gas pressure tests_ D5&D14-v5.doc
Authors	Bertel Nilsson, Mette Amfelt, Christos Tsakiroglou, Tomasz Kasela and Edmund Gosk
Document history	V1- 16.01.2006 V2 – Comments included by Karsten Høgh Jensen, Copenhagen University V3 – QA comments included by Torben O. Sonnenborg, GEUS (04.04.2006)
QA	Torben O. Sonnenborg, GEUS
Status	Final
Target readership	European Commission and Steering Committee
General readership	Project members
Correct reference	Nilsson, B., Amfelt, M., Tsakiroglou C., Kasela, T, Gosk, E. (2006). Results of hydraulic tests performed before and after stimulation of the three test cells in Kluczewo, Poland. Stresoil EU project - Deliverable D5 and D14, April 2006, Geological Survey of Denmark and Greenland, Copenhagen

---

# Table of Content

ABOUT THIS DOCUMENT	2
<b>Table of Content</b>	<b>3</b>
<b>1. Scientific summary</b>	<b>4</b>
<b>2. Introduction</b>	<b>6</b>
2.1 The Stresoil project .....	7
2.2 Scope and objectives .....	8
2.2.1 Task 2-1 Soil mechanics and hydraulic fracture propagation .....	8
2.2.2 Task 2-2 Development of stimulation protocols.....	8
<b>3. Methods</b>	<b>9</b>
3.1 Field instrumentation.....	9
3.1.1 Test Cell 1 (bioremediation) .....	9
3.1.2 Test Cell 2 (hydraulic tests and control) .....	9
3.1.3 Test Cell 4 (steam injection).....	10
3.2 Theoretical methods.....	15
3.2.1 Gas phase permeability (Numerical / Hantush-Jacob) .....	15
3.2.2 Anisotropy of gas phase permeability (Numerical) .....	16
3.2.3 Radius of influence (Theis solution) .....	17
<b>4. Results</b>	<b>18</b>
4.1 Gas injection test before stimulation of Cell 2 (Deliverable D5).....	18
4.1.1 Gas phase permeability and anisotropy .....	18
4.1.2 Radius of influence.....	19
<b>5. Comparison of permeability determined on small intact soil samples and field scale measurements</b>	<b>24</b>
<b>6. Conclusion</b>	<b>27</b>
<b>7. Acknowledgement</b>	<b>28</b>
<b>8. References</b>	<b>29</b>

# 1. Scientific summary

This report summarise the results of hydraulic tests performed before and after stimulation of the three test cells in Kluczewo, Poland. This report was written as part of the STRESOIL EU project - Work Package 3.

Various pressure tests have been performed in the three stimulated cells to determine if change can be observed in the soil hydraulic properties caused by installation of hydraulic fractures. Test results from the bioremediation cell (Cell 1) and the steam injection cell (Cell 4) will be reported in deliverable report D17. Gas phase permeability, anisotropy of gas permeability and radius of influence are determined in Cell 2 to document the change in hydraulic conditions caused by installation of the hydraulic fractures in Cell 2. The gas permeability, anisotropy of gas permeability and radius of influence have been determined prior to and after installation of the hydraulic fractures in Cell 2. Pneumatic air injection tests have been performed in the center wells intersecting the hydraulic fractures at 2.5, 3.5 and 4.5 m depth.

A total of 36 gas phase monitoring wells are placed along a NE-SW and a NW-SE line with bottom of the three fracturing wells in centre of the two crossing lines. The multi-level monitoring wells are placed at the depths 2.5-2.8, 3.5-3.8 and 4.5-4.8 m below ground in clusters at 1.5, 3 and 4.5 m distances away from the center wells.

The Hantush-Jacob analytical solution and trial and error calibrations of the radial numerical code T2VOC have been used to estimate the gas phase permeability and anisotropy of gas permeability in Cell 2. Results indicate that the gas phase permeability ranging between 1.4-2.1 Darcy in SE, SW, NE and NW direction in Unit 2 and between 0.5 and 0.7 Darcy in Unit 3, that means that no significant anisotropy occur in horizontal direction of the gas permeability. In Unit 4 is estimated approximately 0.1-0.2 Darcy in SE direction and 0.6-0.7 Darcy in NW direction, which indicate that the air transmission zone in NW direction is 3-4 times larger than in SE direction.

Gas pressure tests aiming to find radius of influence before stimulating Cell 2 are analysed in analogy to ground water pumping test. Three pressure ranges (0.5, 1 and 1.3-1.5 bar) were used in order to detect an expected growth in the radius of influence in the three pressure steps in the Unit 2-4, but the calculated values indicates that the tests gave ambiguous results. Estimates of radius of influence at 2.5 m depth in Unit 2 indicate pressure propagations in horizontal direction larger than 6m from the injection point. We have only been able to quantify a radius of influence in the NW direction caused by a tendency to increase away from the injection point in the other three directions. This indicates that a great deal of heterogeneity appear in Unit 2. At 3.5m depth (in Unit 3) are radius of influence ranging consistently between 7.2-9.3m in the SE-SW directions at all three pressure stages and again consistently between 16.8-20.5m in the NE-NW direction at the three pressure stages. These results indicate a preferential flow component in the NE-NW direction in a non-stimulated Unit 3. At 4.5m depth (in Unit 4) is the radius values in general showing consistency of calculated radius of influence in the four directions at all three pressure stages. The lowest radius of influence was determined in the SW directions with val-

ues at approximately 5m. In the NW direction the radius of influence is well beyond 7m as in the SE direction where the radius is approximately 8 m. In the NE direction the picture is a bit more confusing with disagreements between the high pressure stage and the two others stages. It is possible the relatively high injection pressure of 1.3 bar has caused the soil to fracture and made a pathway for the air to enter the terrain surface. However, still these results suggest a preferential flow component in the NE direction in Unit 4 before creating the hydraulic fracture as planned.

To summarize the results of the gas injection tests in the three units is it not possible to quantify an increase in the influence radius after establishment of hydraulic fractures at 2.5, 3.5 and 4.5 m depth in Cell 2. However, a substantial change in the air pressure distribution in the total soil volume in Cell 2 has certainly been observed. There are strong indications that the sand-filled fractures have been by-passing the observation points, properly in an upward dipping angel, and that the injected air will travel through the sand-filled fractures to areas of lower permeability zones. This assessment is based on the observation of a substantial decrease in pressure response in basically all the observation points and the slight increase in air-flow rates, after the installation of the fractures.

## 2. Introduction

This report was written as part of the EU project – STRESOIL (Work Package 2, Task 2-4). The report summarise the work done on a detailed study of changes of hydraulic conditions at the refuelling station on Kluczewo airfield, Poland after having stimulated the subsurface with hydraulic fractures. Results of the hydraulic tests performed in test Cell 1, 2 and 4 are reported here. The majority of the work has been done in test Cell 2, where values of bulk gas phase permeability, anisotropy of gas phase permeability and radius of influence are determined. These values are extrapolated to the two test cells 1 (bioremediation) and Cell 4 (steam injection), assuming that the geological heterogeneity is equal for the two remediation cells situated 20-25 m apart from the control Cell 2 (Figure 1).

This report covers the documentation of the following deliverables:

- D5: Results of hydraulic tests in Cell 1 (bioremediation), Cell 2 (control Cell), and Cell 4 (steam injection) prior to the stimulation. The title have been slightly rephrased, since installation of hydraulic fractures in Cell 3 failed due to abandoned obstacles in the subsurface (old waste disposal wells) resulting in severe venting on terrain of propant materials.
- D14: Results of hydraulic tests performed on the stimulated cells.

The report was prepared to support the following milestone:

- M5: Guidelines for establishment of hydraulic fractures at the Kluczewo site.

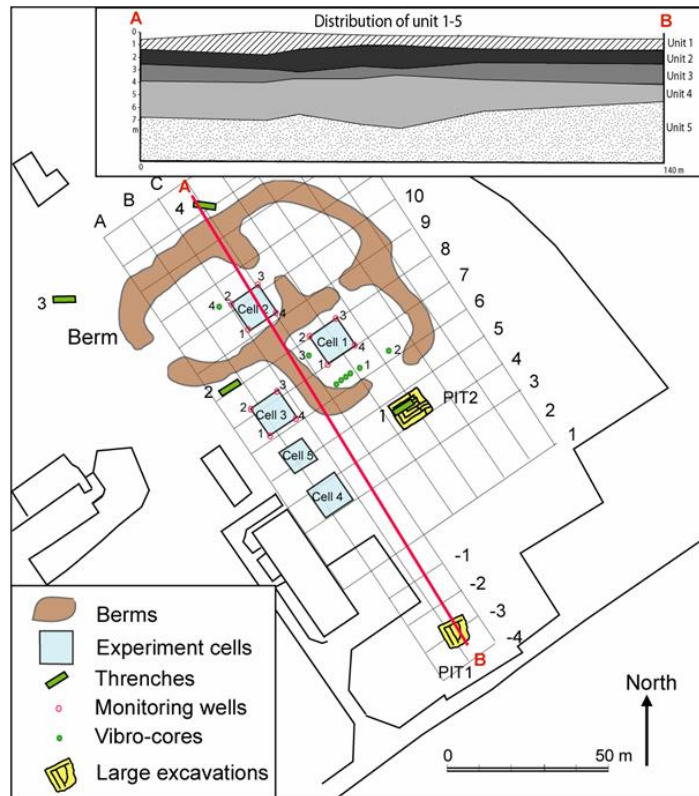


Figure 1. Map of the test site with location of the three test cells (Cell 1, 2, and 4) together with the abandoned Cell 3, pilot Cell 5, and investigation pits and trenches, described in Klint et al (2005).

## 2.1 The Stresoil project

The STRESOIL project (In Situ STimulation and REmediation of contaminated fractured SOILs), Contract Number 004017, is carried out within the Sixth Framework Programme of the European Community ([www.stresoil.com](http://www.stresoil.com)). The “fractured soil” stipulated in the project title is glacial till – one of the most common geological sediments in the European countries. The low permeable, fractured till – while contaminated – represents a great challenge for environmental cleanup procedures. Particularly, if the contamination is present in the unsaturated zone removal of the pollutants becomes very difficult.

A combination of field experiments involving various approaches, laboratory, and investigation of soil and water samples as well as computer simulations will be employed to solve

the problem. A combined effort of a team from Greece, France, Poland, Denmark and USA should within a three years period result in selection of a suitable method for cleanup of the Kluczewo site in NW Poland – the site selected by STRESOIL for field experiments. It is expected that findings of the project will have significant practical applicability in several EU Community countries and else where with same geological setting.

## 2.2 Scope and objectives

The scope of Work Package 2 is to design and install the stimulation technology in three locations at the Polish field site.

The following tasks are specified in WP2:

### 2.2.1 Task 2-1 Soil mechanics and hydraulic fracture propagation

- Simple fracture propagation modelling will be employed
- Geotechnical and textural properties of the glaciogenic clayey deposits will be determined with lab-tests

The reporting of this task contribute to parts of the deliverable D4 (Stimulation protocol)

### 2.2.2 Task 2-2 Development of stimulation protocols

- Combining geotechnical / geological / hydrogeological / NAPL data (WP1) with results of task 2-1 in order to formulate some instructions for the optimal adjustment of the directional permeability in the low permeability soils
- Development of stimulation protocols
- Selection of three locations

The reporting of this task is given in deliverable D4 (Stimulation protocol)

#### Task 2-3 Installation of on-site stimulation set-ups in Cell 1, 2 and 4

- Installation of a number of fractures at three locations. Each set-up will cover an area of approximately 10x10m.

The reporting of this task is given in the deliverable D8 (Installation of on-site stimulation set-ups)

#### Task 2-4 Hydrogeological characterisation of the hydraulic conditions in Cell 1, 2 and 4.

- Performance of hydraulic tests on all three cells prior and after installation of the hydraulic fracture set-ups

The reporting of this task is identical with this report (D5 and D14)

## **3. Methods**

### **3.1 Field instrumentation**

#### **3.1.1 Test Cell 1 (bioremediation)**

Three air leakage tests has been performed by injecting air in each of the pipes used to create the hydraulic fractures at 2.1, 3.6 and 4.2 m depth and observe out flow gas to atmosphere in the two adjacent pipes. Semi-quantitative estimates of gas out flow (leakage) have been obtained by mounting evacuated plastic bags on the injection wells. Additional pressure tests have been carried out in Cell 1a, 1b and 1c (December 2005) to characterise the air flow behaviour in the three non-stimulated and stimulation settings, respectively.

Moreover about 5 m south of Cell 1 a cluster of piezometers is installed in November 2004 by the Dutch drilling company Eijkelkamp for demonstration of the SonicSampDrill system (a vibro core drilling method). These piezometers have been used to obtain understanding of seasonal variations in vertical hydraulic gradients and thickness of the unsaturated zone at the entire field site during the period November 2004 to September 2005 before the remediation activities are started. No gas phase monitoring wells are installed in Cell 1 to avoid inappropriate and uncontrolled oxygen diffusion into the hydrocarbon contaminated soil through the monitoring wells as by-pass flow. It is assumed that the hydraulic parameters determined in Cell 2 are representative for hydraulic conditions at Cell 1 and Cell 4, as well.

#### **3.1.2 Test Cell 2 (hydraulic tests and control)**

Gas phase permeability, anisotropy of gas permeability and radius of influence are determined to document the change in hydraulic conditions caused by installation of the hydraulic fractures in Cell 2. The gas permeability and radius of influence have been determined prior to and after installation of the hydraulic fractures. Various pneumatic air injection tests have been performed in the fracturing wells at 2.5, 3.5 and 4.5 m depth (Table 1).

A total of 36 gas phase monitoring wells placed along a NE-SW and a NW-SE line with bottom of the three fracturing wells in centre of the two crossing lines. The monitoring wells are placed in clusters at the distances 1.5, 3 and 4.5 m from the centre along the two crossing lines. The 12 clusters of 3 wells are placed with bottom of the 30 cm long screens at the depths 2.8, 3.8 and 4.8 m below ground (Figure 2). The diameter of the monitoring wells is ranging between 25-30mm OD and 22-26mm ID. Boreholes were drilled with hand auger equipment (90 mm diameter) gravel packed around the screened section until 5-10 cm above top of screen. The gravel pack was sealed by filling 10 cm of the borehole with a mixture of powdered and granular bentonite that is hydrated with a small volume of water (few ml). The borehole was finally sealed with hydrated cement to the ground surface.

Skin of low permeable materials enveloping a borehole is widely recognised to affect the performance of a Soil Vapour Extraction well. In silty saprolites, which shows hydrological response similar to that observed in low permeable glacial sediments, Bradmer and Mur-

doch (2005) has shown, that the specific capacity correlate to the applied drilling methods. Lowest values are obtained from auger drilling, slightly higher values are given using Shelby tubes, which are normally recommended to be used in low permeable glacial deposits and most reliable results are surprisingly obtained from hand drilled wells. Based on that knowledge it was decided that the gas phase monitoring well in Cell 2 was performed by hand auger drilling.

The field instrumentation of the pneumatic air injection tests is shown in Figure 3. Air pressure at 0.5, 1 and 1.5 bar overpressure was applied one at the time to the three fracturing wells. The pressure response was measured in the monitoring wells at both steady state and transient conditions using U-tube shaped manometers for manual readings and automatic readings using pressure transducers connected to data-loggers (Table 2 & 3). Figure 4 shows a gas pressure response illustrated as piezometric surfaces when injecting air in the intersecting wells connected to the hydraulic fractures in 2.5, 3.5 and 4.5 m depth (all at 1 bar). The “flat” 2.6 m surface suggests that significant air leakage to terrain very likely appears.

### **3.1.3 Test Cell 4 (steam injection)**

Gas pumping tests were conducted in the extraction wells, with the injection wells and cluster of gas phase monitoring wells used as pneumatic piezometers. The well configuration in Cell 4 is shown in Figure 5. Each of the 3 gas pumping tests generated flow rate and pressure measurements at the extraction wells and pressures at injection wells and at the gas phase monitoring wells. These pressure and flow measurements will be used to quantify the pressure distribution and effects of flow between the injection wells and extraction well in each hydraulic fracture by using the numerical code T2VOC. The analyses will be extended to evaluate the expected performance of the combined steam injection and gas extraction experiment in Cell 4. Results of these gas pressure tests will be reported in deliverable report D11 on preliminary simulations for various scenarios of soil remediation.

Table 1. Overview of hydraulic tests performed prior to and after stimulation of the three test Cells 1 (bioremediation), 2 (control Cell) and 4 (steam injection). The hydraulic fractures in Cell 1, 2 and 4 were all installed in May 2005.

Cell	Type of test	Purpose	Period
1	<ul style="list-style-type: none"> <li>Leakage air pressure test in between each fracture well</li> </ul>	(a) Check of by-pass air flow	June and October 2005
	<ul style="list-style-type: none"> <li>Water level measurements in piezometer nest</li> </ul>	(a) Seasonal variations in vertical gradients (b) thickness of unsaturated zone	November 2004 – September 2005
	<ul style="list-style-type: none"> <li>Various pressure gas tests</li> </ul>	(a) Characterisation of air flow behaviour in Cell 1a, 1b and 1c	December 2005
2	<ul style="list-style-type: none"> <li>Air injection tests in all three fractures</li> </ul>	(a) Gas phase permeability (b) Radius of influence (c) Anisotropy of gas phase permeability	May / June 2005
	<ul style="list-style-type: none"> <li>Air injection tests in all three units with fractures</li> </ul>	(a) Gas phase permeability (b) Radius of influence	September / October 2005
	<ul style="list-style-type: none"> <li>Repeated air injection tests in all three units with fractures</li> </ul>	(a) Radius of influence	November 2005
4	<ul style="list-style-type: none"> <li>Leakage air pressure test in fracturing well 2.0, 3.0 and 3.6 m</li> </ul>	(a) Check for by pass air flow between fractures /fracturing wells	June 2005
	<ul style="list-style-type: none"> <li>Gas pumping tests in all three extraction wells</li> </ul>	(a) Determination of hydraulic contact between steam injection wells and extraction wells (b) Testing of remediation equipment in Cell 4 (part of deliverable D14)	October 2005
	<ul style="list-style-type: none"> <li>Vacuum extraction tests in all three extraction wells</li> </ul>	(a) To evaluate vacuum extraction capacity and influence area	November 2005
	<ul style="list-style-type: none"> <li>Air injection in 3 x 3 injection-wells</li> </ul>	(a) To evaluate influence area at steady-state air injection	November 2005

Table 2. Scheme for air injection tests in the three fracturing wells (C2-FRX-2.5; C2-FRX-3.5; C2-FRX-4.5) at three different pressure stages until steady state was reached in all the monitoring wells in Cell 2.

Injection point	Observation points	Pressure (bar)	Pressure (bar)	Pressure (bar)
C2-FRX-2.5	36 monitoring wells	0.5	1	1.3
C2-FRX-3.5	36 monitoring wells	0.5	1	1.5
C2-FRX-4.5	36 monitoring wells	0.5	1	1.3

Table 3. Scheme for air injection tests in the three fracturing wells (C2-FRX-2.5; C2-FRX-3.5; C2-FRX-4.5) at three different pressure stages during transient pressure conditions in five monitoring wells in Cell 2.

Injection point	Observation points	Pressure (bar)	Pressure (bar)	Pressure (bar)
C2-FRX-2.5	C2-G18-2.8	-	1	1.3
	C2-G36-2.8			
C2-FRX-3.5	C2-G17-3.9	0.5	1	1.5
C2-FRX-4.5	C2-G1-4.8	0.5	1	-
	C2-G16-4.8			

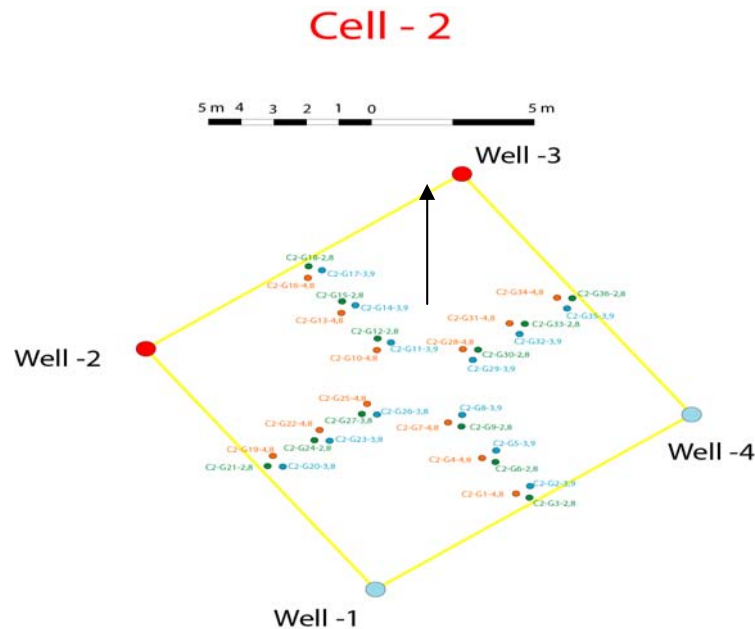


Figure 2. Well configuration of gas phase monitoring wells in test Cell 2 (reference Cell). The fracturing wells can be seen in central part of Figure 2. Arrow shows the North direction.



Figure 3. The field instrumentation of various pneumatic air injection tests performed in Cell 2. Vertical wood boards are the U-shaped manometers for manual readings. The labeling band shows dimensions of the 10 x 10 m test area. The encircled wells are used for gas injection.

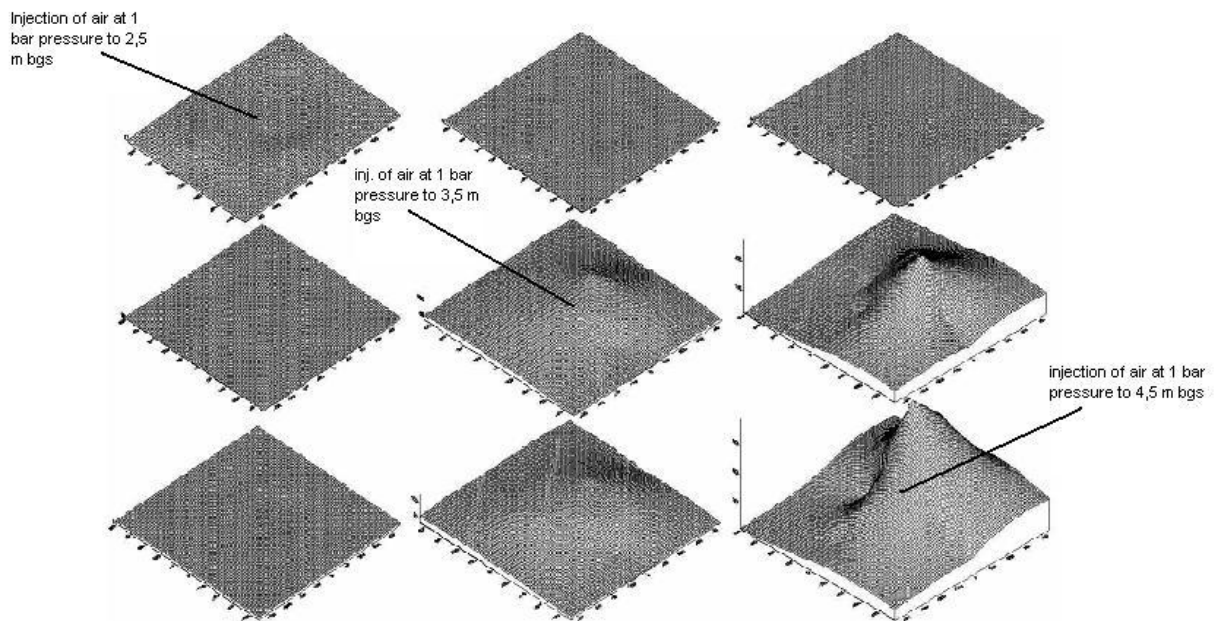


Figure 4. Piezometric surfaces of pressure response at three different depths when injecting air into C2-FRX-2.5; C2-FRX-3.5; C2-FRX-4.5 respectively.

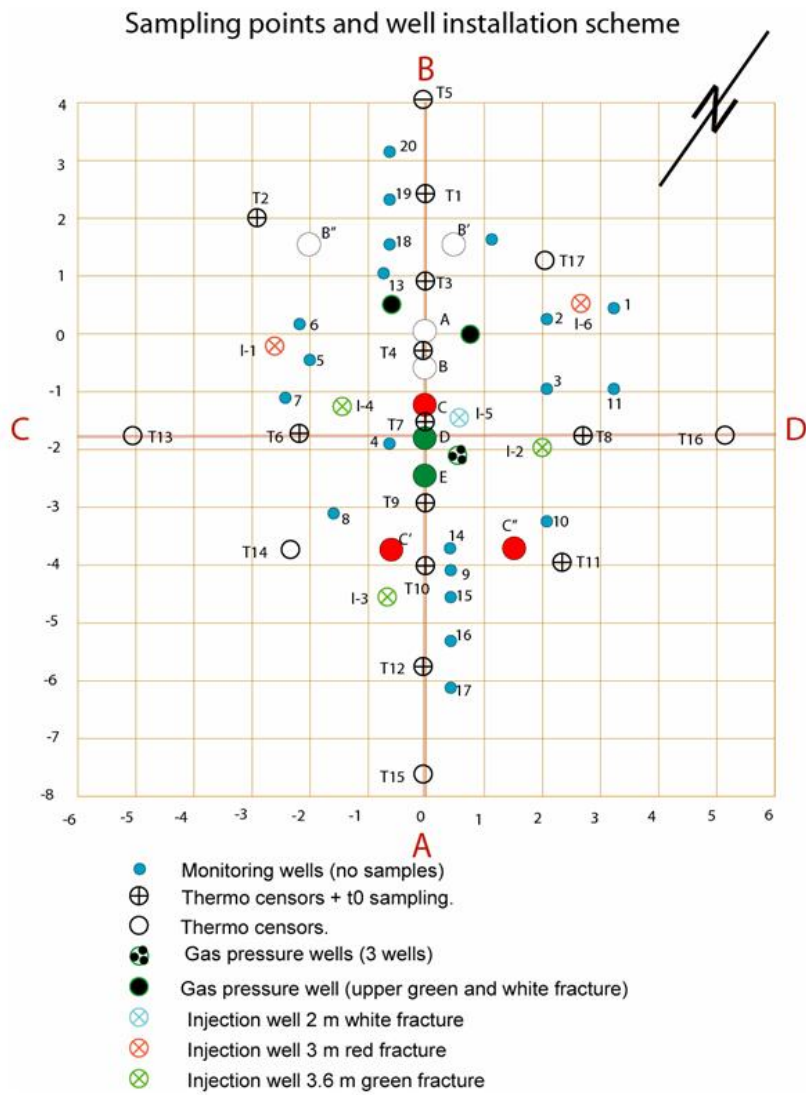


Figure 5. Well configuration in Cell 4 (steam injection).

## 3.2 Theoretical methods

### 3.2.1 Gas phase permeability (Numerical / Hantush-Jacob)

*Hantush-Jacob analytical solution:*

The Hantush-Jacob analytical solution to the flow equation, that takes vertical leakage into account, has been used to calculate the gas phase permeability in Cell 2 before hydraulic fractures was installed. The Hantush-Jacob method is an extension of Theis equation of transient response to vacuum extraction / air injection (Beckett et al., 1994).

$$\Delta H = \frac{Q}{4\pi T} \int_{\left[\frac{r^2 S}{4Tt}\right]}^{\infty} \frac{e^{-x - \left(\frac{r^2}{4B^2 x}\right)}}{x} dx \text{ Where } B = \sqrt{T(b_v/K_v)}, S = \rho g \epsilon b / P_{atm}, T = k \rho g b / \mu$$

B is the vertical leakage factor, S is the storativity of an air-filled system (matrix compressibility is assumed insignificant, Beckett et al., 1994) and T is the transmissivity.

The following Theis assumptions are applied when using the Hantush-Jacob solution: The formation has infinite areal extension, is homogeneous, isotropic and of uniform thickness; The pumping well is fully or partially penetrating the formation; The formation is leaky; Diameter of pumping well is very small so that storage in the well can be neglected; Confining bed(s) has infinite extension of area, uniform vertical hydraulic conductivity and uniform thickness; Confining bed(s) is overlain or underlain by an infinite constant-head plane source flow in the aquitard(s).

Since this method was developed to investigate pressure responses in the same formation as the extraction / injection is conducted, it can not be used to examine pressure responses in adjacent formations. Time dependent pressure measurements were made for at least two pressure stages at two observation wells at the same depth as the air was injected. In Table 4 the scheme for performing the air injection tests is presented. Flow rates were measured and both the pressure responses for air injection and when the air injection stopped were measured as a function of time. The results were analysed as an air pumping test using the aquifer test analysis software AQTESOLV.

Table 4. Scheme of the injection and observation wells used for collecting transient gas pressure data

Injection well	Observation well	Distance (m)	Injection pressure (bar)	Injection pressure (bar)	Injection pressure (bar)	screened (m bgs)
C2-FRX-2.5	C2-G18-2.8	4.7	-	1	1.3	2.5-2.8
	C2-G36-2.8	4.75	-	1	1.3	2.5-2.8
C2-FRX-3.5	C2-G17-3.8	4.4	0.5	1	1.5	3.6-3.9
C2-FRX-4.5	C2-G1-4.8	4.5	0.5	1	-	4.5-4.8
	C2-G16-4.8	4.45	0.5	1	-	4.5-4.8

*Numerical simulation:*

Data from the air injection test given in Table 1 was used to calibrate a 2D radial simulation of the experiment made with the numerical simulation program T2VOC, which can simulate three-phase, three-component, non-isothermal flow of water, air and VOC in three dimensions and in a heterogeneous porous media (Falta et al., 1995).

For simplification some assumptions were made in the construction of the model set-up. It was assumed that the three geological units (Unit 2 – 4) described by Klint et al. (2005) were homogeneous and with constant thickness, which is not the case in reality. Even though the simulation program can simulate multiphase flow, only gas was permitted to flow in this model so the result would be the bulk gas permeability. The model was set up as a 2D radial model with a radius of 10 m. Three units were applied of one meters thickness each. Upper boundary condition was the atmospheric pressure and lower boundary condition was defined by the groundwater table. Initial values were atmospheric pressure in the model area.

Constant air injection pressure was applied to each unit one at a time (as in the experiment) and the gas phase bulk permeability was calibrated by “trial and error” until the best fit to the measured pressure response was obtained for pressure applied to the three units.

### **3.2.2 Anisotropy of gas phase permeability (Numerical)**

The numerical simulation allows for determination of anisotropy that has been calibrated along with the bulk gas phase permeability. This was done in the same model and at the same time as the bulk gas phase permeability was found.

### 3.2.3 Radius of influence (Theis solution)

One of the primary purposes of performing the hydraulic tests in Cell 2 is to determine if there is any change in the soil hydraulic properties after installing hydraulic fractures. Radius of influence of the gas phase is one of these properties. The radius of influence of gas pressure tests are analysed in analogy to ground water pumping test analysis.

An estimate of radius of influence can be found with *the Jacob distance-drawdown method*. Here pressure measurements made at differed distances from the injection point at the same time, are plotted versus the distance (logarithmic scale). At least three pressure measurements should be made in each direction and they should plot on a straight line if the Theis assumptions are fulfilled: the formations are homogeneous and isotropic; constant thickness and infinite radial spreading of the formation; radial symmetric and laminar flow in the zone of transmission; impermeable boundaries above and below the zone of air transmission and insignificant storage within the well bore (Beckett et al., 1994), extraction/injection is conducted in the same formation as the pressure measurements and cannot be used to describe pressure variation in other formations. The intersection between the graph/line and the x-axis (distance) is the radius of influence. To be more precise radius of influence should be interpreted as a parameter that indicates the distance beyond which the drawdown is negligible, or smaller than a certain detection limit.

## 4. Results

### 4.1 Gas injection test before stimulation of Cell 2 (Deliverable D5)

#### 4.1.1 Gas phase permeability and anisotropy

The result of the gas phase permeability was (1) calculated from the transmissivity, which results from curve fitting of the dynamic test solved with the Hantush-Jacob method. The applied parameterisation and the results are given in Table 5. These results indicate that the gas phase permeability ranges between 1.4-2.1 Darcy in SE, SW, NE and NW direction in Unit 2 and between 0.5 and 0.7 Darcy in Unit 3, that means that the horizontal anisotropy is insignificant. In Unit 4 the permeability is estimated to approximately 0.1-0.2 Darcy in SE direction and 0.6-0.7 Darcy in NW direction, which indicate that the air transmission zone in NW direction is 3-4 times larger than in SE direction.

Table 5. Gas phase permeability calculated from transient gas pressure measurements. The Hantush-Jacob analytical solution is including Theis' assumptions and leakage term.

1 Darcy =  $1 \times 10^{-12} \text{ m}^2$

Unit	Injection wells	Observations wells	Direction	Injections pressure (bar)	Flow (l/sec)	Distance (m)	Formation thickness (m)	Transmissivity ( $\text{m}^2/\text{sec}$ )	Permeability (Darcy)
2	C2-FRX-2.5-2.8	G18	NW	1	1.1	4.7	1.9	$2.2 \times 10^{-3}$	2.1
		G36	NE	1	1.1	4.75	1.9	$1.5 \times 10^{-3}$	1.4
3	C2-FRX-3.5-3.8	G17	NW	0.5	0.3	4.4	1	$2.8 \times 10^{-4}$	0.52
		G17	NW	1	1	4.4	1	$3.1 \times 10^{-4}$	0.57
		G17	NW	1.5	2	4.4	1	$3.9 \times 10^{-4}$	0.72
4	C2-FRX-4.5-4.8	G1	SE	0.5	0.4	4.5	3	$3.1 \times 10^{-4}$	0.19
		G1	SE	1	1.7	4.5	3	$1.8 \times 10^{-4}$	0.11
		G16	NW	0.5	0.4	4.45	3	$8.0 \times 10^{-4}$	0.49
		G16	NW	1	1.7	4.45	3	$9.8 \times 10^{-4}$	0.61

(2) The other approach of calculating gas phase permeability is based on trial and error calibrations using the numerical model T2VOC. Results are given in Table 6. Contrary to the analysis carried out above no significant horizontal anisotropy has been found in Unit 4. However, significant heterogeneity in vertical permeability is observed in between the three units with highest contrasts between Unit 2 and 3. Unit 3 and 4 has more similar vertical gas phase permeabilities.

Table 6. Result of the trial and error calibration of the radial numerical model (T2VOC).

Unit	Gas phase permeability $k_x$ (Darcy)	Gas phase permeability $k_y$ (Darcy)	Gas phase permeability $k_z$ (Darcy)
2	1.5	1.5	1.5
3	0.52	0.52	0.01
4	0.21	0.21	0.16

#### 4.1.2 Radius of influence

Calculations of the radius of influence before stimulation based on the Theis analytical solution are shown in Table 7. The radius of influence is obtained by manual graphical readings. Three pressure ranges (0.5, 1 and 1.3-1.5 bar) were used in order to detect a change (i.e. growth) in the radius of influence in the three pressure steps in the Unit 2 to Unit 4, but as the results indicates this gave ambiguous results.

Estimates of radius of influence at 2.5 m depth in Unit 2 indicate pressure propagations in horizontal direction larger than 6m from the injection point. We have only been able to determine a radius of influence values in the NW direction, which indicates that a great deal of heterogeneity appear in Unit 2.

The radius of influence at 3.5m depth in Unit 3 are ranging consistently between 7.2-9.3m in the SE-SW directions at all three pressure stages and again consistently between 16.8-20.5m in the NE-NW direction at the three pressure stages. These results indicate a preferential flow component in the NE-NW direction in a non-stimulated Unit 3.

Evaluation of the radius of influence at 4.5m depth in Unit 4 is in general showing consistency of calculated radius of influence in the four directions at all three pressure stages. The lowest radius of influence was determined in the SW directions with values at approximately 5m. In the NW direction the radius of influence is well beyond 7m as in the SE direction where the radius is approximately 8 m. In the NE direction the picture is a bit more confusing with disagreements between the high pressure stage and the two others stages. It is possible that the relatively high injection pressure of 1.3 bar has caused the soil to fracture and made a pathway for the air to enter the terrain surface. However, still these results suggest a preferential flow component in the NE direction in Unit 4 before creating the hydraulic fracture as planned.

Table 7. Radius of influence given before and after stimulating the cell with hydraulic fractures. \*) Estimate that gives a root mean square error lower than 0.8.

Injection well	Injection pressure (bar)	Direction	Radius of influence (m), <u>before</u>	Radius of influence (m), <u>after</u>
C2-FRX-2.5	1.3	NW	6.0	9.1
C2-FRX-3.5	0.5	SE	8.4	)
		SW	7.4	)
		NW	16.8	)
	1	SE	9.3	9.3
		SW	7.2	6.2
		NW	19.9	23.7
		NE	20.5	18.1
	1.5	SW	7.6	)
		NW	15.8	)
NE		18.3	)	
C2-FRX-4.5	0.5	SW	4.9	)
		NW	7.4	)
		NE	14.1	)
	1	SE	8	)
		SW	5.1	7.4
		NW	7.5	4.1
		NE	21.5	)
	1.3	SW	5.2	)
		NW	5.4	)
NE		6.9	)	

## 4.2 Gas injection test after stimulation (Deliverable D14)

After the hydraulic fractures had been installed in test Cell 2 in the depth of 2.5 m, 3.5m and 4.5m bgs, air injection tests were repeated in the three wells intersecting the fractures. For simplification only 1 bar was added. The result shows a great difference between the pressure response before and after the soil was fractured in all three depths.

Unit 2 showed the smallest changes in pressure response before and after the installation of the hydraulic fracture. Here there was a reduction in pressure response of 50% after the hydraulic fracture was installed. At the same time the injection flow rate was increased to 1.5 l/sec, or 0.4 l/sec higher than before the fractures was made. This suggest that the hydraulic fracture has by-passed all the monitoring points at 2.5m depth (the same depth as the injection point) and the hydraulic fracture is by-passing the injected air the surroundings either out side the test cell or to the soil surface indicated by a constant higher flow rate. The shallow fracture installed in Unit 2 did penetrate the soil surface, which suggests that the hydraulic fracture established in the vicinity of the 32 monitoring points did not create a flat-lying disc but more likely a gently upward dipping sauce shaped feature.

Another important relation that can change the pressure response distribution is the seasonal varying water moisture content in the unsaturated zone. The measurement of the pressure distribution was made in the spring (May 2005; before fracturing) and in the fall (November 2005 ; after fracturing) respectively. Although the soil moisture content was not

measured in the field during the two gas pressure tests it is very likely that this could explain parts of these pressure response differences.

Figure 6 shows a contour plot of the pressure distribution before and after hydraulic fracturing at 2.5m depth in Cell 2. It looks like that the degree of heterogeneity that dominated the highly varied pressure distribution before fracturing, has been more homogeneous indicated by a more evenly distributed pressure response after the hydraulic fractures were installed. Calculations of the radius of influence show an increase from 6 to 9.1m in the NW direction after hydraulic fracturing.

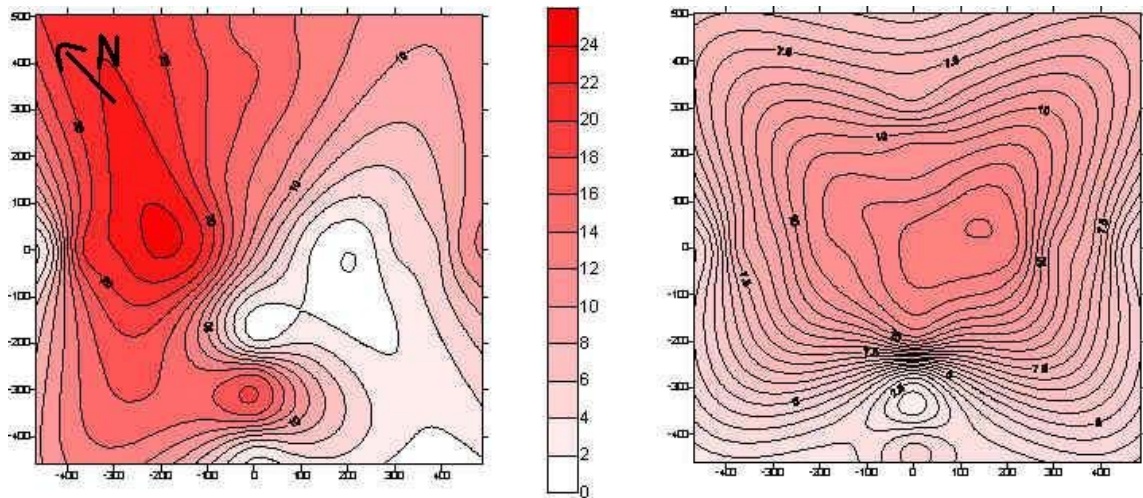


Figure 6. Contour plots of pressure response distribution at 2.5m depth in Cell 2, when injecting air at 1 bar pressure. Left: Pressure response before installing hydraulic fractures. Right: Pressure response after installing hydraulic fracture. Air was injected in the fracturing well at (0,0). Scale in cm H<sub>2</sub>O.

Figure 7 shows the pressure distribution before and after hydraulic fracturing when injecting air at 1 bar pressure at 3.5 m bgs. The two contour maps are similar in geometry but the pressure gradients are much lower after hydraulic fracturing. The difference in the before and after pressure response picture for Unit 3 is quite pronounced, compared with Unit 2. The reductions in pressure gradients are up to 85-90% while injecting air at 1 bar pressure and the flow rate is 1.4 l/sec (before fracturing the flow rate was 1 l/sec at 1 bar pressure). When calculating the radius of influence they are close to the calculations made before fracturing (see Table 7). The significant drop in pressure response and the slightly increased flow rates indicates that the hydraulic fractures have by-passed the observation point and leads the air to the surroundings outside Cell 2 and most likely upward in the formation where the air leaks to the surface or into higher permeable areas in Unit 2.

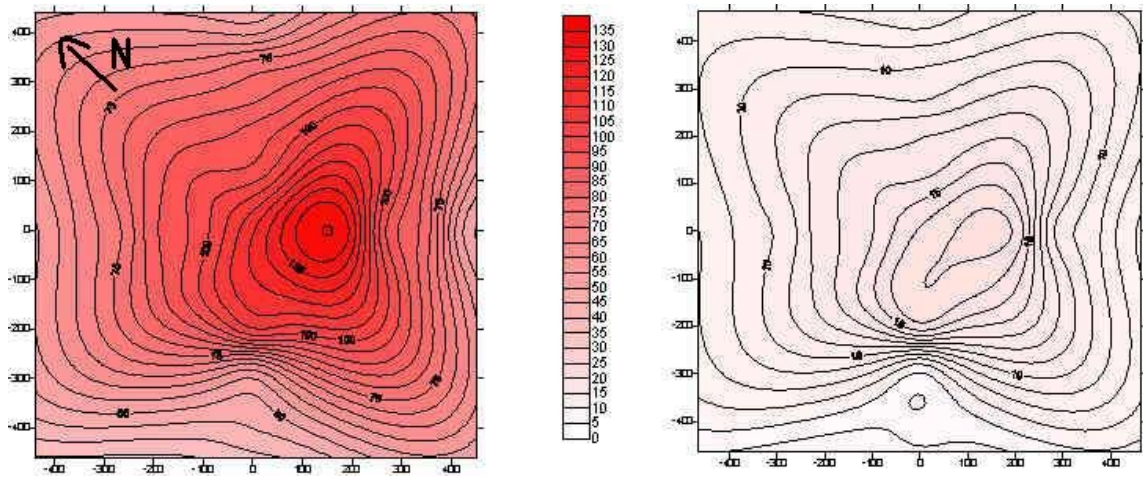


Figure 7. Contour plots of pressure response distribution at 3.5m depth in test Cell 2 when injecting air at 1 bar pressure. Left: Pressure response before installing hydraulic fractures. Right: Pressure response after installing hydraulic fractures. Scale in cm H<sub>2</sub>O.

Figure 8 shows the pressure response distribution at 4.5 m depth in Cell 4 before and after the installation of the hydraulic fractures. The pressure distribution for Unit 4 is a bit different from the two other units. There is a significant difference in the spatial distribution of the pressure and also in the pressure gradients. There is a reduction in the overall pressure distribution, but unlike the two other units, where the pressure drop was almost the same through out the area, here in Unit 4 the reduction is distributed very different from 99% in the NW direction up to 50% increase in the two observation points nearest the injection point in pressure gradients in the NE direction. At the same time the injection flow rate is lower (1.3 – 1.4 l/sec) than before the hydraulic fractures was installed (1.7 l/sec). As the injection of air proceeded there was a slight increase in the flow rate from 1.3 l/sec at the beginning to 1.4 l/sec at the end of the injection period 2 hours later.

So what does this mean? It could mean that most of the observation points have been by-passed by the hydraulic fracture, except for the two observations points nearest the injection point in the NE direction, where there was an increase in pressure after the installation of the fracture, where the fracture has passed through the observation point. The slight increase in the flow rate, during the air injection period, could indicate a slow increase in the gas phase permeability of the formation provided by the water being expelled from the fracture or the surroundings, but since there was no increase in the pressure levels in the observation point it is likely that it is only in the fracture that the water is expelled from, if any.

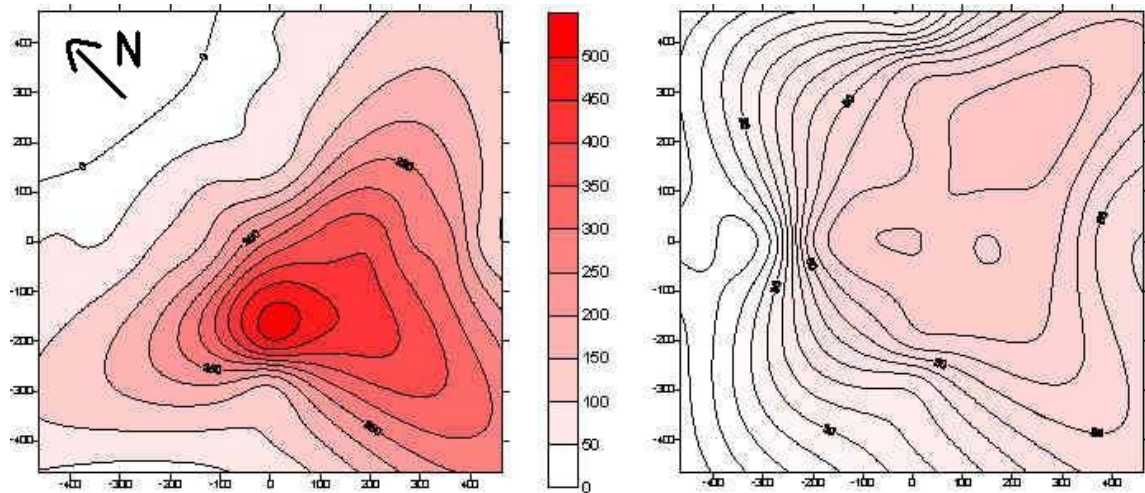


Figure 8. Contour plots of the pressure response distribution at 4.5m depth in test Cell 2 when injecting air at 1 bar pressure in the well at (0,0). Left: Pressure response before installing hydraulic fractures. Right: Pressure response after installing hydraulic fractures. Scale in cm H<sub>2</sub>O.

In summary, the results of the gas injection tests show that the influence radius is not increased after establishment of hydraulic fractures at 2.5, 3.5 and 4.5 m depth. However, a substantial change in the air pressure distribution in the total soil volume in Cell 2 has certainly been observed. Thus there are strong indications that the sand-filled fractures have by-passed the observation points, presumably in an upward dipping angle, and that the injected air will travel through the sand-filled fractures to areas of higher permeability zones. This assessment is based on the observation of a substantial decrease in pressure response in basically all the observation points and the slight increase in air-flow rates, after the installation of the fractures.

## 5. Comparison of permeability determined on small intact soil samples and field scale measurements

The absolute permeability of small soil samples collected during the sampling campaign of September 2004, was measured in a Soxhlet apparatus at FORTH/ICE-HT in Patras, Greece. Each soil sample was cleaned with organic solvents (diethyl-ether, acetone), and packed into a small holder (diameter=3 cm, length=6 cm) in order to measure the absolute permeability and formation factor. It was found that the absolute permeability varies over a broad range of four orders of magnitude ( $1-10^4$  mD) exhibiting sharp variations at the interface of Unit 2 and 3 and within Unit 4 (Figure 9). This is an indication of local heterogeneities caused by the non-uniform spatial distribution of the solid grains with sizes varying in a very broad range (clay, silt, sand, small stones, gravel). The high values of permeability at the interface of Units 2 / 3 and in Unit 4 are associated with the high percentage of small stones of varying size (up to 1 cm) and sand, while the relatively small values of permeability in Unit 3 is due to the high percentage of silt in the soil. Note that an absolute permeability equal to 29 mD was also measured on a long (5cm x 30cm) undisturbed soil sample that was collected from the interface of Unit 3 and 4, and was cleaned in the holder with ethanol /methanol/toluene. The laboratory results will be more thoroughly described in deliverable D23 (Work Package 4).

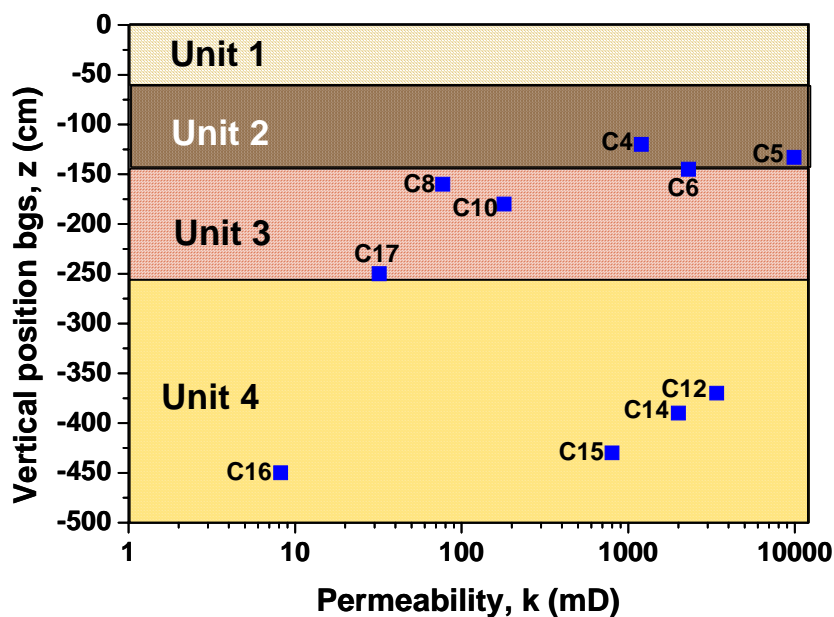


Figure 9. Vertical variation of the absolute permeability over the site (From Stresoil, 2005). Small soil samples collected in Pit 2 (see Figure 1).

The absolute permeability values are not directly comparable with the gas phase permeability determined from the air injection field tests presented in Chapter 4. The absolute permeability is a soil formation characteristic, that strictly describes soil properties, while

the gas phase permeability is a function of the gas content of the formation and the capillary pressure of the formation at a given time and space. The amount of gas present in the formation pore space relatively to the water- and NAPL content is given by a value between 0 and 1. In other words the gas phase permeability is dependent on the soil moisture content and the compositions of the formation at the time of the gas injection in the subsurface.

Capillarity and adsorption are the two forces that retain water in the unsaturated zone (Jensen, 2002) and because of these forces; water will be retained in the smallest pores the longest. So depending on the soil water content, larger pores will be drained first, leaving the residual water isolated in the smallest pores. Thus, if the water content is small (less than 20%) then the water will be retained in the small pores leaving the larger pore spaces connected and available to be occupied by e.g. gas-phase. This means that at water contents of 20% or less is it possible to neglect the residual water contained in the smaller pore spaces and make a direct comparison between values of absolute permeability and gas phase permeability.

Soil moisture content was measured on small soil samples in the same depth as samples were collected for absolute permeability measurements (Figure 9). The soil moisture samples taken in fall 2004 shows a fairly high soil moisture content in Unit 2 of 30-40% decreasing to about 20% at the interface between Unit 2 and Unit 3 and raises to approximately 25% in upper part of Unit 4. The relative high moistures measured can be addressed to rain events at the time of collecting the samples in the field.

The soil moisture content in Unit 2 of 30-40% makes a direct comparison between the absolute permeability determined in the laboratory and the gas phase permeability estimated from field scale tests impossible. It is, on the other hand, possible to say that the gas phase permeability should be smaller than the absolute permeability as a result of the extension of Darcy's law to be valid for multi phase flow where  $k_{\text{gas-phase}} = k_{\text{absolute}} * k_{\text{relative}}$ . The gas phase permeability for Unit 2 was found to be approximately 1.5-2 Darcy, while the absolute permeability values of Unit 2 was ranging between 1.2-9.9 Darcy indicating that the gas phase permeability gives values in the lower end of the absolute permeability interval. If taken into account, that the gas phase permeability is an average (bulk) value of the whole soil volume of Cell 2, then the results from the gas injection test agree quite well with the laboratory estimates.

Unit 3 has a soil moisture content of about 20% that makes it possible to make a direct comparison between the absolute and relative permeability values. Field scale bulk values of 0.5-0.7 Darcy are slightly higher than the absolute permeabilities ranging from 0.03 – 0.18 Darcy. The difference can easily be explained by scaling effects of the different sampling volumes. Unit 3 mainly consists of silt with embedded lenses of sand. The larger field scale values suggest that the main part of the air flow in the field scale experiments will follow more active preferential flow paths through the embedded sand lenses and thereby result in a larger bulk permeability than the permeability obtained from small volume soil samples, that most likely doesn't represent the heterogeneous sandy flow-till system in Unit 3.

Unit 4 is like Unit 3 highly heterogeneous in geological sense and consists mainly of fine silt to fine sand inter-layers of coarse grained sand lenses in a fractured basal till (Klint et al, 2005). This is also evident from the result of the absolute permeability test, where the permeability range from 0.008 to 3.4 Darcy (the high permeability at the top of the unit and then decreasing vertically downward). This could indicate a fining downward facies distribution, which could not be recognized in the geological description for the unit (Klint, et al., 2005).

The gas phase permeability test in Unit 4 gave the range of 0.2 to 0.5 Darcy and with a soil moisture content of 20% at the top of the unit increasing towards the bottom to about 25%. This means, that it is not possible to make the direct comparison of the relative and absolute permeability's in this unit. But when looking at the results, the gas phase permeability lies in the lower end of the range resulting from the absolute permeability test (Table 8), and again according to Darcy's law and the fact that the gas phase permeability is an average over the whole unit, the gas phase permeability should be smaller or lay in the lower end of the absolute permeability.

Table 8. The table shows the measured moist content, the absolute permeability and the gas phase permeability for the three units.

	<b>Moisture content (%)</b>	<b>Absolute permeability (Darcy)</b>	<b>Gas phase permeability (Darcy)</b>
<b>Unit 2</b>	30 – 40	1.2 – 9.9	1.5 – 2.1
<b>Unit 3</b>	20	0.03 – 0.18	0.5 – 0.7
<b>Unit 4</b>	20 – 25	0.0082 – 3.4	0.2 – 0.5

## 6. Conclusion

Air pressure tests have been carried out in Cell 2. Main findings of hydraulic tests performed in Cell 2 can be summarized as follows:

- Gas permeability and anisotropy

The Hantush-Jacob analytical solution and trial and error calibrations of the radial numerical code T2VOC have been used to estimate the gas phase permeability and anisotropy of gas permeability in Cell 2. Results indicate that the gas phase permeability ranging between 1.4-2.1 Darcy in SE, SW, NE and NW direction in Unit 2 and between 0.5 and 0.7 Darcy in Unit 3, that means that no significant anisotropy occur in horizontal direction of the gas permeability. In Unit 4 permeabilities of approximately 0.1-0.2 Darcy in SE direction and 0.6-0.7 Darcy in NW direction are estimated, which indicate that the air transmission zone in NW direction is 3-4 times larger than in SE direction.

After the hydraulic fractures had been installed in test Cell 2 at the depth of 2.5 m, 3.5m and 4.5m bgs, air injection tests were repeated in the three wells intersecting the fractures. For simplification only 1 bar was added. The result shows a great difference between the pressure response before and after the soil was fractured in all three depths.

Unit 2 showed the smallest changes in pressure response before and after the installation of the hydraulic fracture. Here there was a reduction in pressure response of 50% after the hydraulic fracture has been installed. At the same time the injection flow rate was increased to 1.5 l/sec, or 0.4 l/sec higher than before the fractures was made. This suggest that a hydraulic fracture has by-passed all the monitoring points at 2.5m depth (the same depth as the injection point) and that the hydraulic fracture is by-passing the injected air to the surroundings either out side the test cell or to the soil surface indicated by a constant higher flow rate. The shallow fracture installed in Unit 2 did penetrate the soil surface, which suggests that the hydraulic fracture established in the vicinity of the 32 monitoring points did not create a flat-lying disc but more likely a gently upward dipping sauce shaped feature.

- Radius of influence

It is not possible to quantify an increase in the influence radius after establishment of hydraulic fractures at 2.5, 3.5 and 4.5 m depth in Cell 2. However, a substantial change in the air pressure distribution in the total soil volume in Cell 2 has certainly been observed. There are strong indications that the sand-filled fractures have been by-passing the observation points, properly in an upward dipping angel, and that the injected air will travel through the sand-filled fractures to areas of higher permeability zones. This assessment is based on the observation of a substantial decrease in pressure response in basically all the observation points and the slight increase in air-flow rates, after the installation of the fractures.

## 7. Acknowledgement

The present work was carried out within the project In Situ STimulation and REmediation of contaminated fractured SOILs (STRESOIL). The project is funded by The European Commission (Contract Number SSPI-CT-2003-004017) within the Sixth Framework Programme (Global change and ecosystems). In addition this study is part of Mette Amfelt's Master Thesis at Copenhagen University with Prof. Karsten Høgh Jensen as supervisor.

## 8. References

Bradmer, GC and Murdoch, LC (2005). Effects of skin and hydraulic fractures on SVE wells. *Journal of contaminant hydrology*. 77, 271-297.

Beckett, CD and Huntley D (1994). Characterization of flow parameters controlling soil vapour extraction. *Groundwater*, Vol. 32, No. 2. , March-April 1994.

Falta RW, Preuss K, Fintrele S and battistelli A (1995). T2VOC Users's Guide, Lawrence Berkeley laboratory Report LBL-36400, March 1995.

Jensen, K.H., (2002). Soil Physical Processes. Notes for Hydrogeology Class. Geological Institute. University of Copenhagen.

Klint, K.E.S., Kasela, T., Nilsson, B., Haessler, F. (2005). Site description, geological settings and core and soil sampling at the Kluczewo Airport, Poland. Stresoil deliverable D2-D3 report, Geological Survey of Denmark and Greenland. [www.stresoil.com](http://www.stresoil.com)

Stresoil (2005). 1<sup>st</sup> Periodic activity report (Eds. Klint and Nilsson). July 2005. Geological Survey of Denmark and Greenland, Copenhagen.